PHYSICAL REVIEW B VOLUME 15, NUMBER 2 15 JANUARY 1977

Optical absorption of hcp yttrium

J. H. Weaver
Synchrotron Radiation Center, University of Wisconsin, Stoughton, Wisconsin 53589*

C. G. Olson
Ames Laboratory United States Energy Research and Development Administration, Ames, Iowa 50010

(Received 24 May 1976)

The reflectivity of oriented, single-crystal, hcp yttrium was studied in this work between 3.5 and 30 eV. The data were combined with previous absorption measurements at higher and lower energies to enable the dielectric functions to be determined by Kramers-Kronig analysis. Optical anisotropy was shown to occur mainly below 4 eV. The structure in ϵ_2 below 25 eV was interpreted in terms of solid state, interband features. The Y results were compared to earlier results for Zr and Hf. The loss functions were calculated from the dielectric functions, and Y was shown to possess two pairs of surface and volume plasmons.

INTRODUCTION

The electronic properties of the transition metals have come under intense scrutiny in the last few years. Much of the work has emphasized the fcc[1] and bcc[2] metals. The hexagonal metals have received much less attention, and only rarely have oriented, single crystals been investigated by optical techniques.[3,4] Largely because of the dearth of experimental information, there have been few band-structure calculations for these metals.[5] It is hoped that this study of Y will encourage further efforts, both experimental and theoretical, directed at understanding the electronic structure of the noncubic transition metals.

In an earlier paper,[3] we reported the low-energy (0.15–4.4 eV) absorptivity of an oriented, single crystal of Y, but, in the absence of high-energy data on which to base an extrapolation for a Kramers-Kronig analysis, we were unable to determine ϵ_2 and discuss the dielectric-function behavior. Few other studies of Y have been reported. Petrakian *et al.*[6] studied the absorption of thin, semitransparent, films of Y between ~1.5 and 6 eV. Eastman[7] reported ultraviolet photoemission measurements ($\hbar\omega = 11.6$ eV), and indicated an occupied d bandwidth of ~1.6 eV. Electron-energy-loss measurements by Zashkvara *et al.*,[8] Bakulin *et al.*,[9] and Lynch and Swan[10] provided information about the plasmon–dielectric-function mixed structures, but those measurements were unable to separate volume plasmons, surface plasmons, and interband effects. de Haas–van Alphen measurements have recently been reported by Young *et al.*[11] Electronic energy bands have not been calculated for Y but it has been assumed that the Y bands are qualitatively similar to those of Ti, Zr, and Hf, as well as the hcp rare-earth metals. It is only recently that detailed calculations of Ti, Zr, and Hf have appeared.[5]

In this paper, we report our measurements of the reflectivity from 3.5 to 30 eV. Those results were combined with our previous measurements at lower energy[3] and at high energy,[12] and a Kramers-Kronig analysis was performed to yield the dielectric functions. We discuss those results, and calculate the energy-loss functions and oscillator-strength sum rules from them. The loss functions are compared with direct measurements of the energy losses suffered by fast electrons moving through the solid.

In the energy range from 0.15 to 4.4 eV, a calorimetric technique was used as was discussed in greater detail in our earlier paper (Ref. 3); the technique has been extensively discussed in Ref. 13. Briefly, polarized, monochromatic radiation was directed onto the sample at near-normal incidence and absorbed either by the sample or by a Au-black-coated absorber which collected all of the reflected light. The low-energy data were estimated to be accurate to 1% of A ($A = 1 - R$ where R is the reflectivity) above 1 eV, but only 10% of A at 0.15 eV (where A was 0.0229 for $\vec{E} \perp \hat{c}$ and 0.0430 for $\vec{E} \perp \hat{c}$).

Between 3.5 and 30 eV, the room-temperature reflectivity was measured with the same samples. Polarized, continuum radiation from Tantalus I (the 240-MeV electron storage ring operated by the Synchrotron Radiation Center, University of Wisconsin) was used, and the reflectivity was measured by a technique described in detail elsewhere.[14] The data in this energy range were estimated to be accurate to 5% of R. The samples were electropolished, then briefly exposed to the air while being transferred to the vacuum-uv reflectivity chamber. Within 4 min, the pressure in the N_2-purged chamber was ~10^{-3} Torr.

EXPERIMENTAL RESULTS AND DATA ANALYSIS

The reflectivity (R) of Y is shown in Fig. 1 for the energy range between 0.15 and 8 eV. The orientation of the electric field vector of the photon $\vec{E}$, relative to the c axis of the sample is given by $\vec{E} \parallel \hat{c}$ and $\vec{E} \perp \hat{c}$. As was pointed out in Ref. 3, even at the low-energy limit of the data, interband absorption is still quite strong: the Drude or free electron absorption region has not been reached by 0.15 eV in Y, and both interband and intraband effects contribute to the absorption. In the near infrared, the anisotropy in R is striking, and R for $\vec{E} \parallel \hat{c}$ displays structure near 0.5 eV which is not observed for $\vec{E} \perp \hat{c}$. Both spectra reveal features near 1.5 and 2.1 eV. Above ≈ 3 eV, both reflectivities drop sharply, display structure near 5.2 eV (stronger for the basal plane), and have deep minima near 6.4 eV. For $\vec{E} \parallel \hat{c}$, $R = 0.002$ at the minimum. While considerable anisotropy is apparent in R below about 4 eV, at higher energy the two reflectivities run nearly parallel and show little anisotropy.

In Fig. 2, the reflectivities are shown for the region between 5 and 28 eV. Here, the extent of the minima near 6.4 eV is shown more clearly than in Fig. 1. Above 6.4 eV, R rises sharply, displays features at about 7.8 eV (shoulder), 10.2 eV (maximum), 11.8 eV (shoulder), 14.7 eV (minimum), 18.5 and 23 eV (broad maxima), 27.2 eV (minimum), and is rising at 28 eV. It should be borne in mind that the two curves shown are the measured reflectivities and, as such, include angle of incidence (10°) and polarization effects. For $\vec{E} \parallel \hat{c}$, the radiation was s polarized, while for $\vec{E} \perp \hat{c}$, it was p polarized. This, rather than a physical anisotropy, accounts for much of the difference in the magnitude of R in Fig. 2. The dependence of R on polarization and angle of incidence has been discussed in more detail in Ref. 14 and elsewhere. For the present discussion, we need only point out that the Kramers-Kronig computer program takes both factors into account before performing the integration routine and ultimately determining the dielectric function.

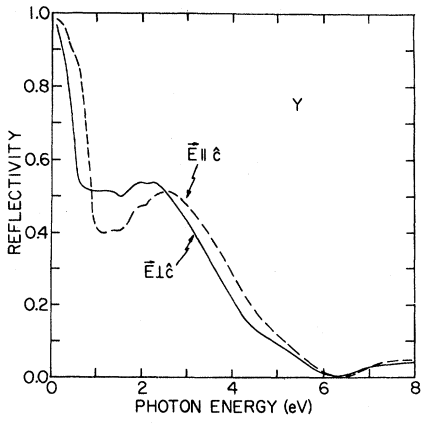

FIG. 1. Reflectivity of Y to 8 eV emphasizing the low-energy anisotropy of hcp Y.

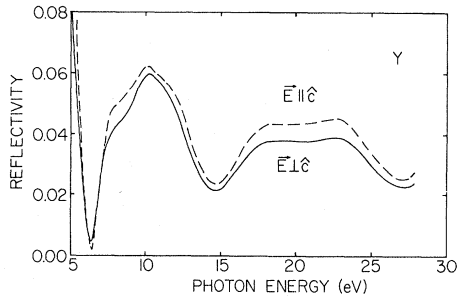

FIG. 2. Reflectivity of Y at high energy. The curve labeled $\vec{E} \parallel \hat{c}$ was taken at 10° angle of incidence with s-polarized light; the $\vec{E} \perp \hat{c}$ data were also taken at 10° but with p-polarization radiation.

In order to gauge the effect of an oxide on the sample, one sample was aged. (This was accomplished by measuring R for the sample in an "as-is" state; it had been electropolished some 25 months earlier, then stored in a glass vial.) The effect of the surface layer was to fill in the minimum near 6.4 eV and push it toward lower energy. In addition, the magnitude of R was higher, additional structure was observed at 13.3 eV, and the minimum near 15 eV was completely filled in. Electropolishing removed the oxide, and, though a surface layer formed during the mounting and pump-out process, the effect was primarily a filling-in of the minimum near 6.4 eV and a distorting of the feature near 7.8 eV.

As a further check of our Y data, we measured the reflectivity of a large crystal of $Y_{33}O_{48}$. The spectrum of the oxide crystal was very different from that shown in Fig. 2. In particular, the oxide sample showed maxima in R at 7 and 12.6 eV with magnitudes of R everywhere above 20% between 6.3 and 13.3 eV. The Y reflectivity was much lower—its maximum at 10.2 eV was only 6%. Above 13 eV, the oxide spectrum was relatively flat and $\approx 5\%$.

As a final set of measurements, we evaporated a film of Y *in situ* in a chamber with a base pressure of 2×10^{-9} Torr. Subsequent measurements showed the film to have considerably more resemblance to the oxide crystal than the crystal of Y. Since Y is highly reactive when hot and exhibits strong gettering, we were forced to conclude that a film evaporated in a chamber with anything less than state-of-the-art vacuum would not show structures representative of the well-ordered metallic

state.

In order to determine the dielectric functions from the R data, a Kramers-Kronig analysis was performed with the present data and those of Refs. 3 and 12 forming a continuous curve from 0.15 to 250 eV. A Drude-like behavior was assumed in the infrared, and an exponential behavior of the form $R = R_0 E^{-\beta}$ was taken above 250 eV. Several values of β were assumed, and the ultimate choice of $\beta = 3.5$ was influenced primarily because of considerations of the sum rule on N_{eff}.

The real and imaginary parts of the dielectric function are shown in Fig. 3. The low-energy region ($\hbar\omega$ less than 4 eV) is expanded for clarity. Note that the energy scale is linear, but changes at 4 eV, and that above 4 eV, the quantities shown are $10\epsilon_2$ and $10\epsilon_1$. For ease in comparing the results for the two polarizations, the zero line for ϵ_1 has been displaced from that of ϵ_2. As indicated above in the discussion of the reflectivity, the principal anisotropy occurs below about 4 eV. Structure which occurs in ϵ_2 is summarized for both polarizations in Table I.

The optical conductivity, defined by $\sigma = \epsilon_2 \omega / 4\pi$, is shown for Y in Fig. 4. The advantage of the figure is that the low-energy features are shown more clearly—in particular, note the structure near 0.43 for $\vec{E} \perp \hat{c}$ which is apparent in σ but barely visible in ϵ_2 (Fig. 3).

TABLE I. Energy locations of structure in ϵ_2 for Y. Energies are given in eV.

$\vec{E} \parallel \hat{c}$	$\vec{E} \perp \hat{c}$
~0.4 [a]	0.74
1.35	1.15
1.78	1.75
~2.2 [b]	~2.2 [b]
~5.2 [b]	~5.2 [b]
7.7 [b]	7.7 [b]
10.2	10.2
11.6	11.6
18.3 [c]	18.3
~22.5 [c]	~22.5

[a] Weak structure, better seen in the conductivity (Fig. 5).
[b] Shoulder.
[c] Broad feature.

DISCUSSION

In general, the evaluation of low-energy optical data calls for a careful study of the electronic energy bands of the material. Structure in the data is correlated to pairs of bands, separated by the correct energy difference, which have a high joint density of states, and which are allowed by group-theoretical selection rules. It is also important in the case of metals to realize that structure can arise from transitions occurring over an extended volume of k space, and that the principal regions of k space contributing to a particular structure can be removed from the high symmetry points or lines often calculated. To definitively relate experimental structure to regions of k space requires a careful consideration not only of the bands but also of the wave functions, the dipole matrix elements, and then eventually ϵ_2.

In the present consideration of Y, the interpretation is hampered because the bands from which the arguments must be made are those of Zr. Nevertheless, those bands are very instructive and are reproduced as Fig. 5. They were calculated by Jepsen *et al.*[5] who used a linear muffin-tin-orbital formalism and included relativistic and spin-orbit effects. To determine the location of the Fermi

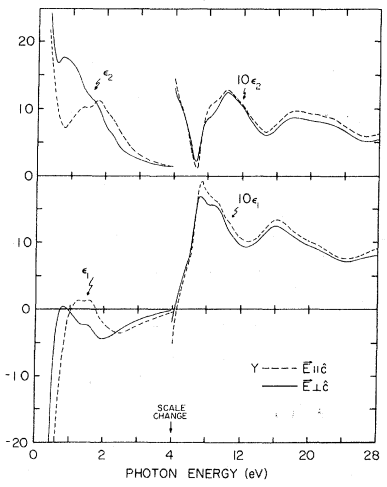

FIG. 3. Dielectric function for Y. The zero line has been displaced for clarity and to emphasize the differences and similarities for the two polarizations. The energy scale is linear but changes at 4 eV.

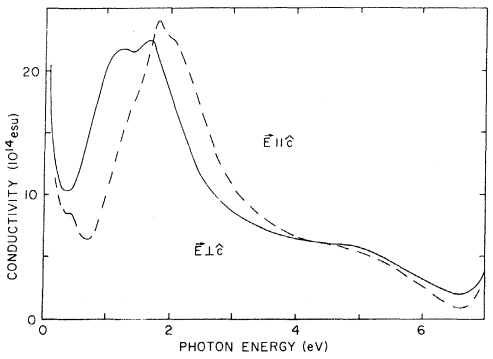

FIG. 4. Optical conductivity of Y below 6 eV.

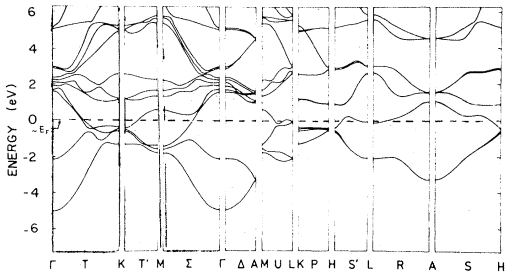

FIG. 5. Electronic energy bands of Zr calculated by Jepsen *et al.* (Ref. 5), including spin-orbit and relativistic effects. The dashed line represents the Fermi level of Y determined by using the density of states of Zr. Its position should be taken cautiously.

level appropriate for Y, but in the Zr bands, we have assumed that the density of states is unchanged on going from Zr to Y. This is not a completely valid assumption, and in fact the width of the d bands of Y is expected to be appreciably narrower than in Zr, but it allows a rough interpretation of the low-energy optical structures in Y. The Fermi level as we have shown it was determined by assuming three electrons per atom and using the Zr density of states.

Experimental structure in ϵ_2 and σ is observed near 0.43 eV (see Fig. 4) for $\vec{E} \| \hat{c}$ but not for $\vec{E} \perp \hat{c}$. There are few pairs of bands which could be responsible for the structure. We suggest that transitions like $\Sigma_3 \rightarrow \Sigma_1$ and $T_2 \rightarrow T_1$ are involved; these are allowed for $\vec{E} \| \hat{c}$ but are forbidden for $\vec{E} \perp \hat{c}$.

The experimental structure observed for $\vec{E} \perp \hat{c}$ at 0.74 eV can probably be related to transitions near H along the direction S'. Such $S_1' \rightarrow S_1'$ transitions are allowed by selection rules.

Structure is evident for both polarizations between 1 and 2 eV, but it is difficult to make unambiguous assignments of the origin of the structure without detailed matrix element calculations. The importance of selection rules is also difficult to assess except at the lowest energies. The structure in ϵ_2 near 1.75 eV in both polarizations may, for example, originate from the same part of the zone but be distorted by anisotropy in the absorption at lower energy. This would not be unreasonable since the calculations of Jepsen *et al.*[5] have shown that most of the bands are hybridized to some extent throughout the zone (only specific points retain a pure angular momentum character). A possible source for the structure near 1.75 eV might then be the nearly parallel bands along T and T' extending out from K (the Zr bands show too small an energy separation but the Y bands would be expected to be farther apart).

In the absence of detailed calculations, one can only suggest that the regions of k space along P (1.3–1.5 eV for Zr bands) and near the zone face around M and along P (2.8–3 eV) are probably contributing to interband absorption in Y.

A comparison of the spectra of Fig. 3 with the corresponding behavior in Zr and Hf shows considerable resemblance above ~5 eV. Each of the metals possesses a sharp minimum in ϵ_2 near 6 eV (Y, 6.6; Zr, 6.2; Hf, 6.8 eV); broad absorption persisting for several electron volts; a second minimum (Y, 14.8; Zr, 17.2; Hf, 18.9 eV); and a third, broad, double-structured feature to ~30 eV. These features can be interpreted qualitatively in terms of transitions from the occupied levels to regions of relatively high density of states many eV above E_F. For several of the bcc and fcc metals, it has been demonstrated that structure appears in the density of states well above E_F, and it appears reasonable to assume that the corresponding bands would persist in the hcp metals. In particular, Christensen[15] has performed relativistic-augmented-plane-wave calculations for Au to ~50 eV above E_F, and the bands are decidedly not free-electron-like. Unfortunately, more quantitative arguments cannot be made until thorough calculations have been performed which focus attention on the high-lying states of the hcp metals.

The energy loss functions for Y can be calculated easily from the dielectric functions shown in Fig. 4. These functions are measures of the probability that a fast electron will excite a surface ($\mathrm{Im}[-1/(\tilde{\epsilon}+1)]$) or volume ($\mathrm{Im}(-1/\tilde{\epsilon})$) plasmon as it moves through the crystal. Since the dielectric functions for Y show little anisotropy above about 4 eV, we show in Fig. 6 the energy loss functions for only the one polarization, $\vec{E} \perp \hat{c}$. Strong features are observed in the volume loss function at 5.2 and 12.4 eV, and we identify those as volume

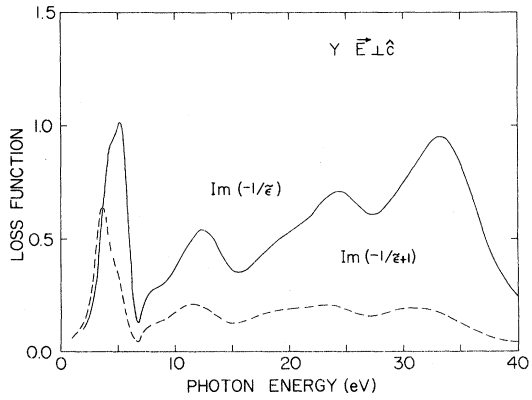

FIG. 6. Energy-loss functions for Y. The volume-loss function is $\mathrm{Im}(-1/\tilde{\epsilon})$ and the surface-loss function is $\mathrm{Im}[-1/(\tilde{\epsilon}+1)]$.

plasmons since the conditions are satisfied that $d\epsilon_1/dE > 0$; $d\epsilon_2/dE < 0$; $\epsilon_1 \approx 0$ and ϵ_2 small and structureless. Other features in the volume loss function can be identified as interband features since they correspond to structure in either ϵ_1 or ϵ_2. Since strong interband absorption occurs near 12 eV, it is not surprising that the plasmon at that energy is broadened and shifted in energy away from the calculated free-electron value of 11.18 eV. The corresponding distortion of the surface plasmon is even greater, and its energy position is uncertain (~11.5 eV). The lower-energy surface plasmon is, however, strong and occurs at 3.75 eV.

Most measurements which directly measure the losses of electrons transmitted by thin foils or reflected from bulk surfaces have been unable to separate volume from surface-plasmon effects.[16] They have observed, nevertheless, structures at energies which are close to those where our optical constants place plasmons. The work by Lynch and Swan[10] reported structure at 4.0, 12.4, 35.6, 49.1, and 74.1 eV. The first could be a mixture of our low-energy plasmon pair, and the second corresponds well to our volume plasmon. The structures at 25.4 and 35.6 eV correspond to our bulk peaks at 24.5 and 33.2. We have no explanation for the feature near 25 eV, but the structure at 33.2 eV is due to the $4p \rightarrow 4d$ absorption as discussed in Ref. 12.

Finally, a comparison of the reflectivity spectra of Fig. 3 with the absorption measurements of Ref. 12 shows that the reflectivity curves fail to display the onset on the atomic $4p$-$4d$ absorption near 23 eV. A similar behavior has been observed in Zr and Hf. We believe the disagreement arises because of the relative strengths of the interband absorption and the atomic absorption, the interband structure obscuring the weaker atomic features in the crystalline sample but the atomic structure showing more clearly in the films. As we noted earlier, Y films, even those prepared in uhv, tend to be contaminated and hence interband features would be weakened. Features such as the broad $4p$ structures would be less affected since they are a result of localized absorption on the metal atom and are largely independent of the atomic environment.

ACKNOWLEDGMENTS

The authors gratefully acknowledge the continued support of E. M. Rowe (Director, SRC) and D. W. Lynch. Correspondence with O. K. Andersen was beneficial.

---

*Supported by NSF Grant No. DMR74-15089.

[1]For a review of the optical properties of Rh, Pd, Ir, and Pt, see J. H. Weaver, Phys. Rev. B 11, 1416 (1975). Additional data are available in J. H. Weaver and R. L. Benbow, *ibid.* 12, 3509 (1975) [Pd] and J. H. Weaver, C. G. Olson, and D. W. Lynch [Ir] (unpublished).

[2]See the following and references therein: J. H. Weaver, D. W. Lynch, and C. G. Olson, Phys. Rev. B 7, 4311 (1973) [Nb]; 10, 501 (1974) [V, Mo, Ta]; 12, 1393 (1975) [W]; and 14, 459 (1976) [V, Nb, Cr, Mo]; Solid State Commun. 16, 163 (1975) [Mo].

[3]J. H. Weaver and D. W. Lynch, Phys. Rev. B 7, 4137 (1973) [Y].

[4]D. W. Lynch, C. G. Olson, and J. H. Weaver, Phys. Rev. B 11, 3617 (1975) [polycrystalline Ti, Zr, Hf].

[5]O. Jepsen, O. K. Andersen, and A. R. Mackintosh, Phys. Rev. B 12, 3084 (1975) [Zr, Hf, Os, Ru]; and O. Jepsen, Phys. Rev. B 12, 2988 (1975) [Ti].

[6]J. P. Petrakian, J. P. Palmari, and G. Rasigni, Appl. Opt. 9, 2115 (1970).

[7]D. E. Eastman, Solid State Commun. 7, 1697 (1969).

[8]V. V. Zashkvara, M. I. Korsunskii, V. S. Red'kin, and V. E. Masyagin, Fiz. Tverd. Tela 11, 3667 (1969) [Sov. Phys.-Solid State 11, 3083 (1970)].

[9]E. A. Bakulin, L. A. Balabanova, M. M. Bredov, E. G. Ostroumova, E. V. Stepin, and V. V. Shcherbinina, Fiz. Tverd. Tela 11, 685 (1969) [Sov. Phys.-Solid State 11, 549 (1969)].

[10]M. J. Lynch and J. B. Swan, Aust. J. Phys. 21, 811 (1968).

[11]R. C. Young, R. G. Jordan, D. W. Jones, and V. J. Hems, J. Phys. F 4, L84 (1974).

[12]For additional work with the transition metals in the soft-x-ray region, see J. H. Weaver and C. G. Olson [Y, Zr, Nb, Mo, Rh, Pd, Hf, and W] Phys. Rev. B 14, 3251 (1976) and references therein.

[13]L. W. Bos and D. W. Lynch, Phys. Rev. B 2, 4567 (1970).

[14]C. G. Olson and D. W. Lynch, Phys. Rev. B 9, 3159 (1974).

[15]N. E. Christensen, Phys. Rev. B 13, 2698 (1976).

[16]Wehenkel and Gauthé have reported results for many transition metals which separate volume, surface, and interband effects. See, for example, C. Wehenkel and B. Gauthé, Phys. Lett. A 47, 253 (1974) and Opt. Commun. 11, 62 (1974). They have not yet reported such results for Y though they have measured the energy losses in Y and Y_2O_3 (private communication).